Journal of Hydrology 575 (2019) 1200–1213

Contents lists available at ScienceDirect

Journal of Hydrology

journal homepage: www.elsevier.com/locate/jhydrol

Research papers

Hybrid models to improve the monthly river flow prediction: Integrating artificial intelligence and non-linear time series models

Farshad Fathian[a], Saeid Mehdizadeh[b,*], Ali Kozekalani Sales[c], Mir Jafar Sadegh Safari[d]

[a] Department of Water Science & Engineering, Faculty of Agriculture, Vali-e-Asr University of Rafsanjan, P.O. Box 77188-97111, Rafsanjan, Iran
[b] Department of Water Engineering, Urmia University, Urmia, Iran
[c] Department of Civil Engineering, Elm-o-Fan University College of Science and Technology, Urmia, Iran
[d] Department of Civil Engineering, Yaşar University, Izmir, Turkey

ARTICLE INFO

This manuscript was handled by G. Syme, Editor-in-Chief

Keywords:
ANN
MARS
RF
SETAR
GARCH
Monthly river flow
Canada

ABSTRACT

Prediction of river flow as a fundamental source of hydrological information plays a crucial role in various fields of water projects. In this study, at first, the capabilities of two time series analysis approaches, namely self-exciting threshold autoregressive (SETAR) and generalized autoregressive conditional heteroscedasticity (GARCH) models, then three artificial intelligence approaches including artificial neural networks (ANN), multivariate adaptive regression splines (MARS), and random forests (RF) models were investigated to predict monthly river flow. For this purpose, monthly river flow data of Brantford and Galt stations on Grand River, Canada, for the period from October 1948 to September 2017 were used and their performances were evaluated based on various evaluation criteria. The SETAR model showed better performance than the GARCH one in prediction of river flows at the stations of study. Additionally, the stand-alone MARS and RF models performed slightly better than the ANN. Next, hybrid models were developed by coupling the used ANN, MARS, and RF models with SETAR and GARCH models as the non-linear time series models. The performance of various models presented in this study indicated that the new hybrid models demonstrated a much better performance compared with the stand-alone ones at both stations. Among the developed hybrid models, the RF-SETAR models generally had the best accuracy to improve the river flows modeling. As a result, it can be concluded that the presented methodology can be used to predict hydrological time series such as river flow with a high level of accuracy.

1. Introduction

An accurate estimation of river flows in watersheds and water resources systems plays a major role for more timely and efficient management of water projects. Furthermore, having information on the river flows is needed to manage rivers, flood warning systems and especially, planning for optimal operations. River flow modeling seems to be a complex process due to the impacts of hydro-climatic variables such as evaporation, temperature, precipitation, etc. on river flow. There are commonly two approaches in estimation of river flows, which can be classified in two groups of physically-based (or conceptual) and mathematically-based (or data-driven) models (Gershenfeld and Weigend, 1994; Peueot et al., 2003; Babovic, 2005; Di et al., 2014; He et al., 2014; Zhang et al., 2016). The physically-based models are complex and need complicated mathematical tools, sufficient physical data, and some extent of expertise and experience with the models that impede the application of these types of models (Aqil et al., 2007; He et al., 2014). While data-driven models are simpler to implement, not so complex and they do not require any information on the physical nature of hydrological processes. As these models are popular and commonly used for modeling hydrological processes; therefore, they can be helpful and valuable for modeling river flows (Chau et al., 2005; Nayak et al., 2005; Wu et al., 2009; He et al., 2014).

Artificial intelligence approaches as one of the data-driven models are able to model hydrological processes using only a series of input data although they may have some disadvantages; for example, they do not include any physical parameters. Additionally, non-considering the stochastic component of hydrological variables along with the deterministic component obtained by these models can be another disadvantage of these methods. Accordingly, it seems that the use of these models alone cannot be an appropriate approach in modeling the hydrologic time series. In such circumstances, artificial intelligence

* Corresponding author.
E-mail addresses: f.fathian@vru.ac.ir (F. Fathian), saied.mehdizadeh@gmail.com (S. Mehdizadeh), jafar.safari@yasar.edu.tr (M.J.S. Safari).

https://doi.org/10.1016/j.jhydrol.2019.06.025
Received 18 April 2019; Received in revised form 28 May 2019; Accepted 9 June 2019

Table 1
Detailed information of the previous studies reviewed in this research.

References	River	Location	Scale	Models used	Best model
Yu et al. (2004)	Tryggevælde catchment and Mississippi	Denmark and USA	Daily	Chaos, Naive, Inverse, ARIMA, EC-SVM	EC-SVM
Kisi and Cimen (2011)	Canakdere and Goksudere	Turkey	Monthly	SVR, W-SVR	W-SVR
Samsudin et al. (2011)	Selangor and Bernam	Malaysia	Monthly	GLSSVM, GMDH, LSSVM, ANN, ARIMA	GLSSVM
Sanikhani and Kisi (2012)	Garzan and Bitlis	Turkey	Monthly	ANFIS-SC and ANFIS-GP	ANFIS-SC
Kalteh (2013)	Navrood and Shafarood	Iran	Monthly	ANN, W-ANN, SVR, W-SVR	W-SVR
Awchi (2014)	Zab	Iraq	Monthly	FFNN, GRNN, RBFNN, MLR	FFNN
Terzi and Ergin (2014)	Kızılırmak	Turkey	Monthly	AR, GEP, ANFIS, RBFNN, FFNN	AR
Zhang et al. (2016)	Wuding	China	Annual	AR, RBFNN, EMD-RBFNN, EMD-RBFNN-Polynomial, CEREF	CEREF
Yaseen et al. (2016a)	Tigris	Iraq	Monthly	ELM, SVR, GRNN	ELM
Ghorbani et al. (2016a)	Zarrinehrud	Iran	Monthly	SVM, MLP, RBFNN	MLP and RBFNN
Yaseen et al. (2016b)	Johor	Malaysia	Daily	RBFNN, FFNN	RBFNN
Ghorbani et al. (2016b)	Big Cypress	USA	Daily	SVM, ANN, MLR, RC	ANN
Ravansalar et al. (2017)	Beshar	Iran	Monthly	W-LGP, LGP, ANN, W-ANN	W-LGP
Moeeni et al. (2017)	Jamishan	Iran	Monthly	SARIMA, ANFIS, ANN, SARIMA-ANFIS, SARIMA-ANN	SARIMA-ANFIS
Fathian et al. (2019)	ZarrinehRood	Iran	Daily	VAR, VAR-MGARCH	VAR-MGARCH

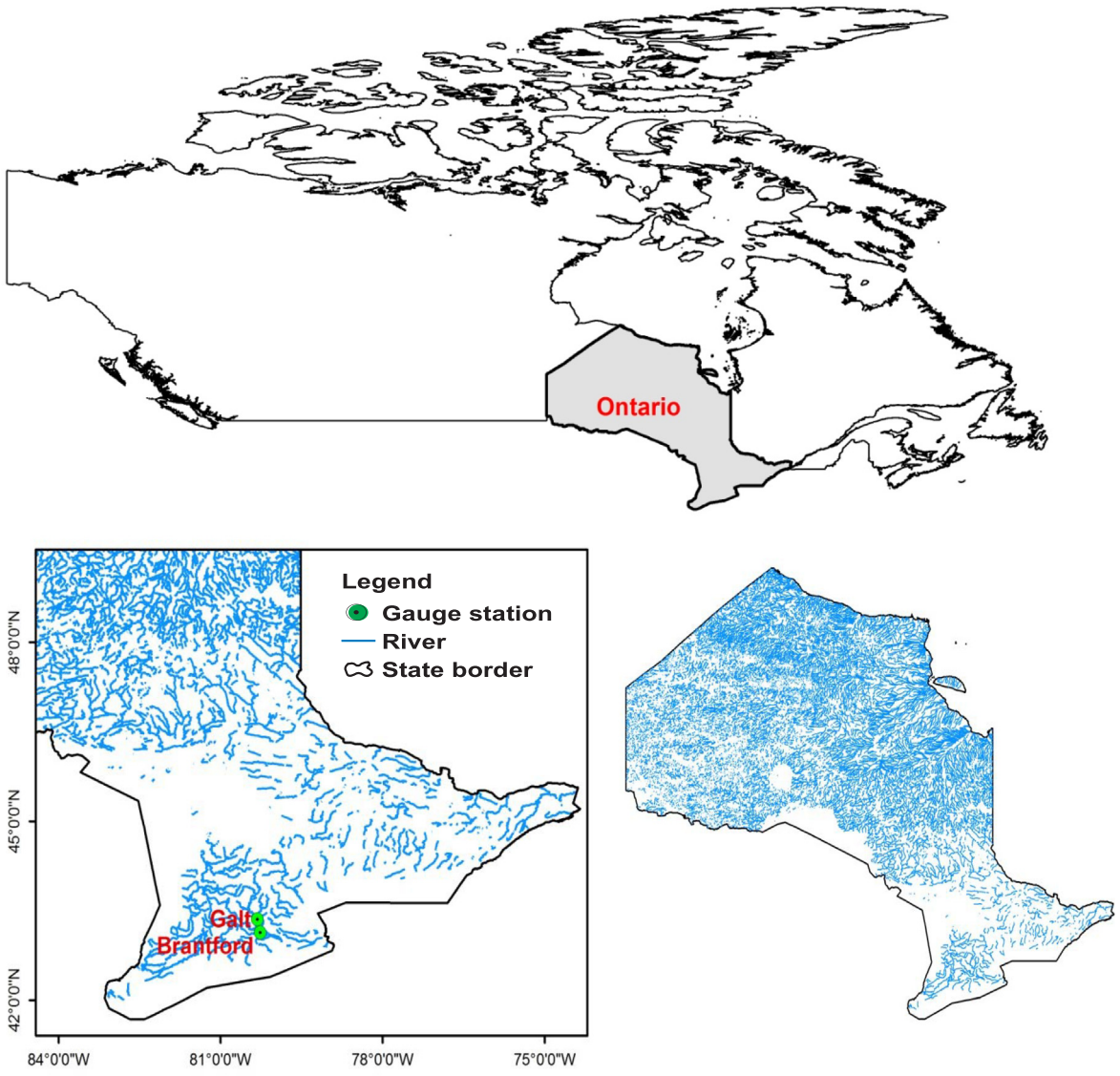

Fig. 1. The geographical position of the studied stations in Southwestern Ontario, Canada.

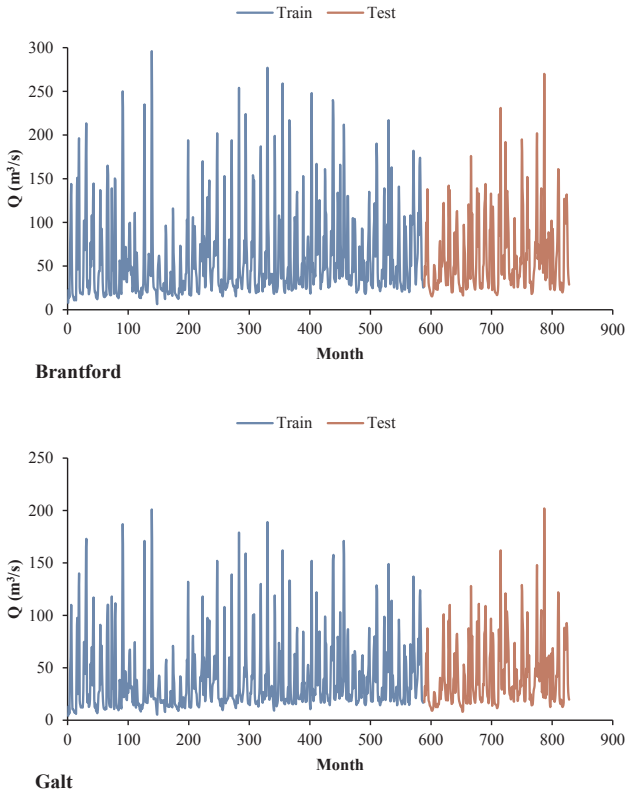

Fig. 2. Time series of the observed monthly river flow data for the studied stations during the train and test periods.

models coupled with the time series models, can be taken into account for hydrological processes, instead of using single models.

During recent decades, artificial intelligence models have being extensively applied to predict hydrologic time series such as streamflow. Artificial neural networks (ANN), multivariate adaptive regression splines (MARS) and random forests (RF) are three kinds of these models. Yu et al. (2004) introduced a hybrid model by combining the chaos theory and support vector machine (SVM), namely EC-SVM for daily runoff forecasting of Tryggevælde catchment, Denmark and the Mississippi River at Vicksburg. The proposed EC-SVM hybrid model was found to be better than other methods used including standard chaos, naive, inverse, and autoregressive integrated moving average (ARIMA). Kisi and Cimen (2011) evaluated the performance of wavelet-support vector regression (W-SVR) and single SVR for monthly streamflow prediction at Canakdere and Goksudere rivers, Turkey. The results revealed that the proposed W-SVR presented better performance than the stand-alone SVR to predict streamflow. Samsudin et al. (2011) predicted monthly river flow of Selangor and Bernam rivers, Malaysia, using group method of data handling (GMDH) coupled with the least squares support vector machine (LSSVM) named as GLSSVM, single GMDH, and LSSVM as well as ANN and ARIMA models. It was concluded that the new hybrid model (i.e., GLSSVM) had the best accuracy in comparison with the other models. Sanikhani and Kisi (2012) employed two different types of adaptive neuro-fuzzy inference system (ANFIS), namely grid partitioning (ANFIS-GP) and subtractive clustering (ANFIS-SC) for modeling monthly river flow at Garzan and Bitlis streams, Turkey. The results of this study uncovered that the ANFIS-SC outperformed the ANFIS-GP. Kalteh (2013) used the ANN and SVR techniques combined with wavelet transform for predicting monthly river flow of Kharjegil and Ponel stations, Iran. The results showed that the single SVR had slightly better accuracy compared with the single ANN. Awchi (2014) forecasted monthly river discharge of Bakhma and Dokan sites on the Upper and Lower Zab River in Northern Iraq,

Table 2
Statistical parameters of the monthly river flow data for the studied stations in each dataset.

Station	Dataset	Min (m^3/s)	Max (m^3/s)	Mean (m^3/s)	S_x (m^3/s)	C_s	C_v
Brantford	Train	6.39	296.00	58.62	49.55	1.88	0.85
	Test	15.50	270.00	61.77	43.48	1.53	0.70
	Whole	6.39	296.00	59.53	47.87	1.80	0.80
Galt	Train	4.19	201.00	38.85	34.10	2.06	0.88
	Test	7.92	202.00	42.05	31.47	1.65	0.75
	Whole	4.19	202.00	39.77	33.37	1.95	0.84

Min, Max, Mean, S_x, C_s and C_v denote the minimum, maximum, mean, standard deviation, coefficient of skewness and coefficient of variation of the monthly river flow data, respectively.

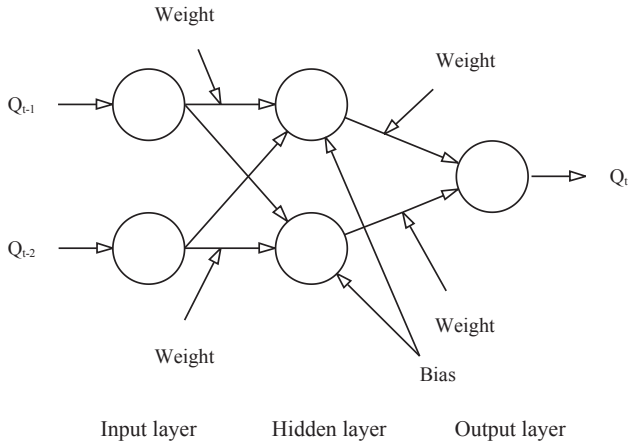

Fig. 3. Architecture of the ANN used to predict monthly river flow (e.g. ANN2 at Brantford and Galt stations).

Table 3
Input combinations used to develop the different models.

Models	Input combinations	Output
ANN1, MARS1, RF1	Q_{t-1}	Q_t
ANN2, MARS2, RF2	Q_{t-1}, Q_{t-2}	Q_t
ANN3, MARS3, RF3	Q_{t-1}, Q_{t-2}, Q_{t-3}	Q_t

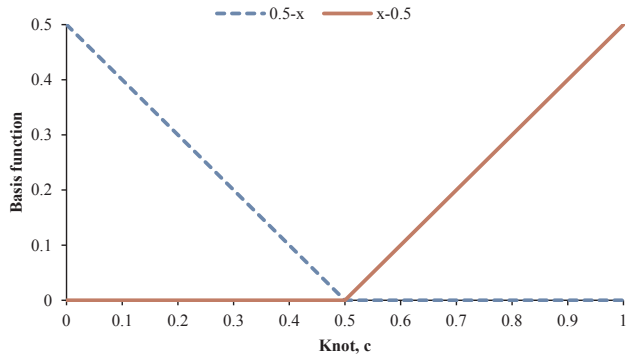

Fig. 4. The basis function chart at $c = 0.5$.

respectively, using feed forward neural networks (FFNN), generalized regression neural networks (GRNN), radial basis function neural networks (RBFNN), and multiple linear regression (MLR). It was found that the FFNN outperformed the other used models. Terzi and Ergin (2014) employed autoregressive (AR) time series model as well as gene expression programming (GEP), RBFNN, FFNN, and ANFIS for predicting monthly river flow of Kızılırmak River, Turkey. They reported that the

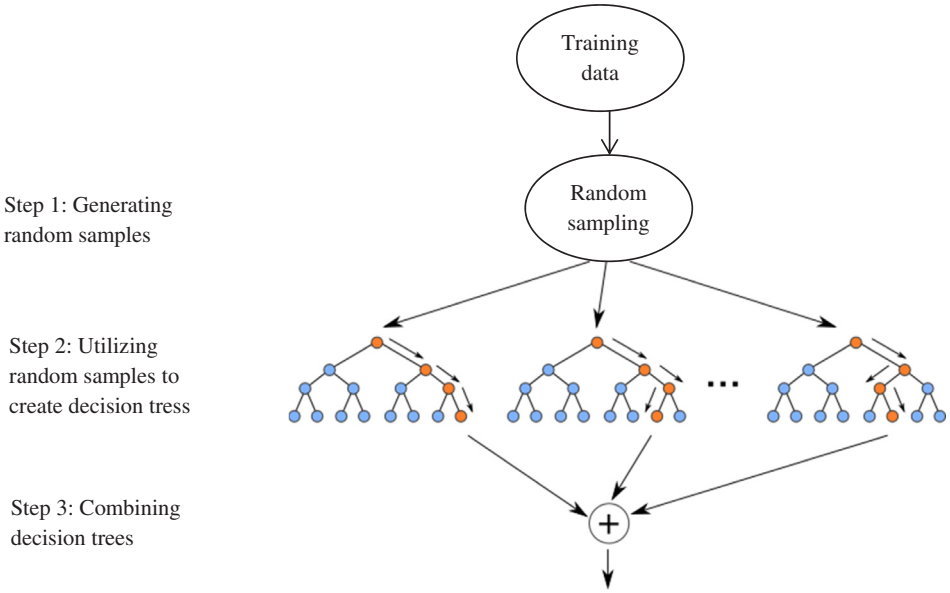

Fig. 5. The general structure of RF model.

Table 4
Equations obtained by the SETAR and GARCH models at the studied stations.

Station	Models	Equations	
Brantford	SETAR (1,1)	$Q_t = \begin{cases} -0.0555 + 0.4352 * Q_{t-1} \\ 0.1443 + 0.2750 * Q_{t-1} \end{cases}$	if $Q_{t-2} \le 0.4057$ if $Q_{t-2} > 0.4057$
	GARCH (1,0)	$\sigma_t^2 = 0.62119 + 0.26513 * \varepsilon_{t-1}^2$	
Galt	SETAR (1,1)	$Q_t = \begin{cases} -0.0549 + 0.4190 * Q_{t-1} \\ 0.1037 + 0.2862 * Q_{t-1} \end{cases}$	if $Q_{t-2} \le 0.3792$ if $Q_{t-2} > 0.3792$
	GARCH (1,0)	$\sigma_t^2 = 0.59565 + 0.32837 * \varepsilon_{t-1}^2$	

AR model performed the best; in addition, the GEP and ANFIS had higher accuracy than the RBFNN and FFNN. Zhang et al. (2016) introduced a hybrid model, namely CEREF, which is an integration of empirical mode decomposition (EMD), RBFNN, and external forces (EF) variable. They concluded that the suggested CEREF model can be considered as a suitable and alternative approach to predict annual streamflow of Wuding River Basin. Yaseen et al. (2016a) conducted a comparative study among extreme learning machine (ELM), GRNN, and SVR for monthly streamflow prediction in the Tigris River, Iraq. The ELM model was found to be better than the SVR and GRNN ones. Ghorbani et al. (2016a) predicted monthly river flow of some hydrometric stations on Zarrinehrud River, Iran, using multilayer perceptron (MLP), SVM, and RBFNN. The results showed that the predictions of RBFNN and MLP were better than the SVM. The forecasting performance of FFNN and RBFNN models were assessed by Yaseen et al. (2016b) for daily river flow at Johor River, Malaysia. The superiority of the RBFNN over the FFNN was reported in this study. Ghorbani et al. (2016b) modeled daily river discharge by the SVM, ANN, conventional MLR and rating curve (RC) approaches for Big Cypress River, Texas, USA. Performance evaluation of models revealed that peak values of river discharge modeled by the ANN and SVM models were more accurate than those obtained by the MLR and RC. Ravansalar et al. (2017) introduced wavelet-linear genetic programming (W-LGP) to model the monthly streamflow at Pataveh and Shahmokhtar stations located on Beshar River, Iran. Furthermore, the W-LGP model performance was evaluated in comparison with the single ANN, LGP, wavelet-ANN (W-ANN), and MLR. The results revealed that the proposed W-LGP model had the highest accuracy at the studied regions. Moeeni et al. (2017) used seasonal ARIMA (i.e., SARIMA) integrated with ANFIS and ANN methods for monthly inflow prediction. The results presented that the hybrid SARIMA-ANFIS model is the superior model among all. Fathian et al. (2019) employed the multiple linear (VAR: Vector Auto-Regressive) and nonlinear (DVECH: Diagonal Vectorization Heteroscedasticity) time series models in modeling daily streamflow process. The results demonstrated that the hybrid VAR-DVECH has better performance than the VAR model. Some of detailed information on previous studies reviewed in this study is summarized in Table 1.

Among many time series models developed for modeling hydrological time series, two models namely, SETAR (self-exciting threshold autoregressive) and GARCH (generalized autoregressive conditional heteroscedasticity) were used in the present study. These models are as the new non-linear types of time series models, which have not widely been used to modeling hydrological processes (Komorník et al., 2006; Modarres and Ouarda, 2013).

This research attempts to predict monthly river flow of Brantford and Galt stations situated on Grand River, Canada. In this regard, the aims of this study are: (1) to assess the accuracy of the stand-alone SETAR, GARCH, ANN, MARS, and RF models for predicting monthly river flow, (2) to develop hybrid models by coupling the ANN, MARS,

Table 5
Error statistics of the time series models at Brantford and Galt stations during the train and test periods.

Station	Models	Train				Test			
		RMSE (m^3/s)	MAE (m^3/s)	R^2	E	RMSE (m^3/s)	MAE (m^3/s)	R^2	E
Brantford	SETAR(1,1)	14.73	10.69	0.913	0.911	14.13	10.64	0.895	0.894
	GARCH(1,0)	16.00	11.22	0.908	0.896	16.07	12.17	0.877	0.863
Galt	SETAR(1,1)	10.08	7.30	0.915	0.912	10.25	7.59	0.895	0.894
	GARCH(1,0)	11.17	7.72	0.908	0.892	11.55	8.66	0.880	0.865

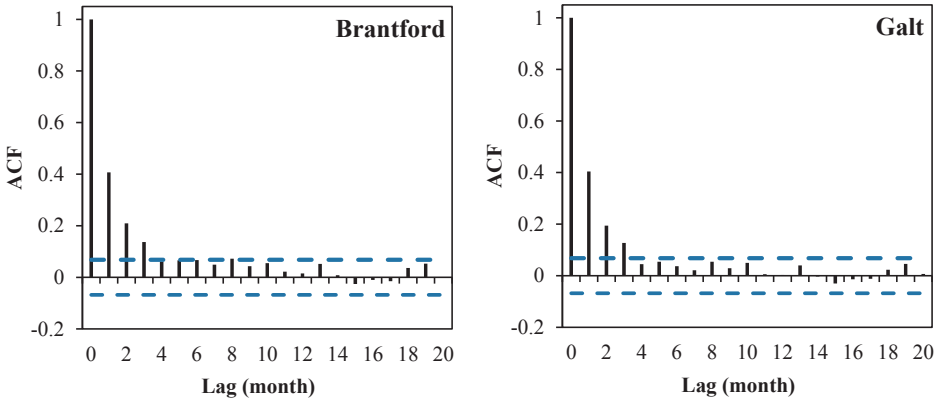

Fig. 6. The ACF graphs of the standardized river flow datasets at the studied stations.

Table 6
Error statistics of the stand-alone and the corresponding hybrid models at Brantford during the train and test periods.

Models	Train				Test			
	RMSE (m^3/s)	MAE (m^3/s)	R^2	E	RMSE (m^3/s)	MAE (m^3/s)	R^2	E
ANN1	34.53	22.32	0.515	0.513	34.64	24.43	0.400	0.363
ANN2	35.75	21.95	0.486	0.479	35.78	24.86	0.383	0.320
ANN3	35.12	22.14	0.498	0.497	34.90	24.81	0.408	0.353
ANN1-SETAR	5.88	3.39	0.986	0.986	**8.37**	**6.33**	**0.975**	**0.963**
ANN2-SETAR	6.49	4.44	0.988	0.983	9.05	6.87	0.969	0.956
ANN3-SETAR	4.47	2.62	0.993	0.992	8.87	7.13	0.979	0.958
ANN1-GARCH	8.01	4.89	0.979	0.974	10.75	7.35	0.961	0.939
ANN2-GARCH	9.41	6.71	0.975	0.964	10.81	7.82	0.963	0.938
ANN3-GARCH	8.24	5.18	0.979	0.972	10.85	7.83	0.971	0.937
MARS1	35.00	22.75	0.500	0.500	34.07	23.02	0.409	0.383
MARS2	34.73	22.34	0.508	0.508	33.16	22.49	0.439	0.416
MARS3	33.47	21.69	0.543	0.543	32.38	21.85	0.461	0.443
MARS1-SETAR	4.14	2.94	0.994	0.993	**4.07**	**2.89**	**0.991**	**0.991**
MARS2-SETAR	6.54	4.26	0.984	0.983	5.24	4.05	0.987	0.985
MARS3-SETAR	10.24	5.27	0.965	0.957	8.51	5.45	0.966	0.962
MARS1-GARCH	8.18	5.11	0.982	0.973	7.78	5.39	0.975	0.968
MARS2-GARCH	9.08	6.03	0.978	0.966	8.84	6.43	0.973	0.958
MARS3-GARCH	13.67	7.76	0.953	0.924	11.97	8.27	0.947	0.924
RF1	34.65	22.45	0.510	0.510	32.93	22.47	0.444	0.424
RF2	34.06	21.80	0.529	0.527	32.22	21.74	0.461	0.448
RF3	33.84	22.47	0.534	0.533	32.39	22.23	0.455	0.443
RF1-SETAR	5.65	3.94	0.988	0.987	5.99	4.26	0.983	0.981
RF2-SETAR	5.31	3.27	0.989	0.989	**4.95**	**3.37**	**0.988**	**0.987**
RF3-SETAR	5.77	3.93	0.989	0.986	5.37	3.95	0.987	0.985
RF1-GARCH	9.87	6.07	0.973	0.960	9.96	6.71	0.963	0.947
RF2-GARCH	9.18	5.63	0.975	0.966	9.66	6.44	0.963	0.950
RF3-GARCH	9.82	6.11	0.974	0.961	9.83	6.82	0.964	0.949

Bold values denote the error statistics of the best hybrid models at test period.

and RF models with SETAR and GARCH models, and (3) to compare the accuracy of river flow modeling by the hybrid models proposed in this study with the stand-alone ones. It can be noted that the hydrological time series like river flow is comprised of stochastic and deterministic components. It is worthwhile to be expressed that according to the authors' knowledge, the stochastic component of river flow has not usually been considered in the previous studies through the non-linear time series models. However, in this study, the stochastic components of river flow data were considered in the modeling procedure. On the other hand, recent works on modeling the hydrological variables such as river flow have focused on the separate application of artificial intelligence and time series models. However, the use of artificial intelligence models is more than the time series models in hydrological modeling. In contrast, the application of hybrid artificial intelligence-time series models in literature for hydrological parameters modeling is significantly less than for the stand-alone artificial intelligence and time series models. Besides, few studies have been reported in literature to consider the stochastic behavior of river flow in modeling procedure by the time series models in coupled with the artificial intelligence techniques through the hybrid artificial intelligence-time series models. Therefore, this study as an innovation investigates the abilities of the ANN, MARS, and RF models coupled with the non-linear SETAR and GARCH time series models in predicting monthly river flow.

2. Materials and methods

2.1. Study area and data used

The present study was carried out for two hydrometric stations, namely Brantford and Galt situated on Grand River in Canada. The Grand River, as a large river in Southwestern Ontario, Canada, with length of 280 km, is entirely within southern Ontario's boundaries and it flows southwards to Lake Erie (https://www.grandriver.ca/en/index.aspx). The geographical location of study area is demonstrated in Fig. 1. The monthly river flow data were acquired from the official website of the Government of Canada (https://wateroffice.ec.gc.ca) with the

Table 7
Error statistics of the stand-alone and the corresponding hybrid models at Galt during the train and test periods.

Models	Train				Test			
	RMSE (m^3/s)	MAE (m^3/s)	R^2	E	RMSE (m^3/s)	MAE (m^3/s)	R^2	E
ANN1	24.75	15.20	0.478	0.472	25.75	17.74	0.350	0.328
ANN2	24.55	15.77	0.481	0.481	26.35	18.94	0.365	0.296
ANN3	24.94	15.35	0.465	0.464	26.49	18.64	0.343	0.288
ANN1-SETAR	4.57	2.62	0.985	0.982	**5.22**	**4.14**	**0.980**	**0.972**
ANN2-SETAR	3.59	2.13	0.990	0989	8.15	6.68	0.977	0.933
ANN3-SETAR	3.64	2.31	0.989	0.989	7.18	5.88	0.975	0.948
ANN1-GARCH	6.24	4.10	0.973	0.966	7.44	5.33	0.960	0.944
ANN2-GARCH	6.58	4.01	0.976	0.963	9.82	7.37	0.965	0.902
ANN3-GARCH	6.39	4.09	0.974	0.965	8.94	6.63	0.960	0.919
MARS1	24.75	15.76	0.473	0.472	25.56	16.89	0.365	0.338
MARS2	24.28	15.45	0.492	0.492	24.88	16.45	0.393	0.372
MARS3	23.93	15.39	0.507	0.507	24.15	16.18	0.422	0.409
MARS1-SETAR	2.59	1.81	0.995	0.994	**2.50**	**1.79**	**0.995**	**0.994**
MARS2-SETAR	5.35	3.30	0.979	0.975	5.32	3.41	0.975	0.971
MARS3-SETAR	7.42	4.03	0.960	0.953	6.30	4.28	0.967	0.960
MARS1-GARCH	6.26	3.77	0.979	0.966	6.03	3.99	0.974	0.963
MARS2-GARCH	6.95	4.64	0.975	0.958	7.74	5.39	0.959	0.939
MARS3-GARCH	9.43	5.46	0.951	0.923	8.88	6.08	0.949	0.920
RF1	24.15	15.37	0.497	0.497	24.74	16.53	0.399	0.380
RF2	24.02	15.12	0.505	0.503	24.12	15.94	0.422	0.410
RF3	23.76	15.71	0.516	0.514	24.32	16.60	0.414	0.400
RF1-SETAR	4.15	2.77	0.987	0.985	4.01	2.93	0.987	0.984
RF2-SETAR	3.50	2.07	0.990	0.989	**3.54**	**2.31**	**0.989**	**0.987**
RF3-SETAR	4.13	2.86	0.989	0.985	4.34	3.08	0.987	0.981
RF1-GARCH	7.22	4.45	0.971	0.955	7.07	4.83	0.968	0.949
RF2-GARCH	6.60	4.11	0.974	0.963	6.92	4.73	0.967	0.952
RF3-GARCH	7.32	4.42	0.972	0.954	7.45	5.20	0.967	0.944

Bold values denote the error statistics of the best hybrid models at test period.

length of 828 monthly data (from October 1948 to September 2017). In order to train the models, the first 588 data (about 71% of the total data) of river flow time series (from October 1948 to September 1997) for each station was used. In addition, the data between October 1997 and September 2017 (240 months; about 29% of the total data) were employed in test stage. Fig. 2 illustrates the observation time series plot of monthly river flow data for both stations throughout the studied period. The statistical properties of the river flow time series are presented in Table 2. As clear, generally, similar statistical parameters are observed for both train and test periods.

It is better to mention that the observed river flow time series must be standardized due to the use of time series models (i.e., SETAR and GARCH) for predicting river flows as well as to eliminate the dimension of observational river flow datasets. Herein, whole monthly river flow datasets of the studied stations were standardized through the following equation:

$$Q_s = \frac{Q_o - \bar{Q}_o}{\sigma_{Q_o}} \tag{1}$$

where Q_s, Q_o, $\bar{Q}_o$, and σ_{Q_o} denote the standardized river flow data, observed river flow data, the mean of observed data, and the standard deviation of observed data, respectively (Mehdizadeh et al., 2019).

2.2. ANN model

The ANN is the biologically inspired approach, which is widely used to estimate complex and non-linear systems. In the ANN, the relationships between input and output variables are simulated by inspiration from the human brain features. In general, an ANN model is composed of three layers and as an example, the structure of the ANN model used in the present study is illustrated in Fig. 3. The first layer is the input layer that receives the input information. The hidden layer is the information processing sector. The last layer is the output layer that receives the processed information from the previous layer and then gives the final output. Moreover, each layer consists of processor units called neurons. The general form of an ANN can be expressed as:

$$y = f\left(\sum_{i=1}^{n} x_i w_i + b_i\right) \tag{2}$$

where y is the output, x_i denotes the input vector (i = 1,2, …, n), w_i is the weight vector, b_i is the bias and f is the transfer (activation) function.

In this research, in order to predict the river flow data, feed forward back propagation neural networks having three-layer were applied. Input layer is composed of different combinations of lagged monthly river flow data (see Table 3). The same input and output variables were considered for the MARS and RF models. The hidden layer plays a significant role to achieve high performance by the ANN. Therefore, using trial and error method, the optimal numbers of neurons were acquired for the hidden layer. Training the ANN is in fact to adjust the values of network parameters consisting of weights between input and hidden layers as well as between hidden and output layers and biases between the hidden and output layers. Moreover, the functions used in the hidden and output layers were, respectively, tangent-sigmoid and linear transfer functions.

2.3. MARS model

The MARS as a non-parametric regression approach was presented by Friedman (1991) to reveal hidden non-linear pattern in datasets with a large number of variables. This model is based on functions named basis functions, which are defined as follows:

$$\begin{cases} \max(0, x - c) \\ \max(0, c - x) \end{cases} \tag{3}$$

where x is the input and c is a constant, which is called knot. These basis functions (Eq. (3)) are known as spline functions being in fact a reflected pair at c knot (Fig. 4). The general form of the MARS can be defined as below:

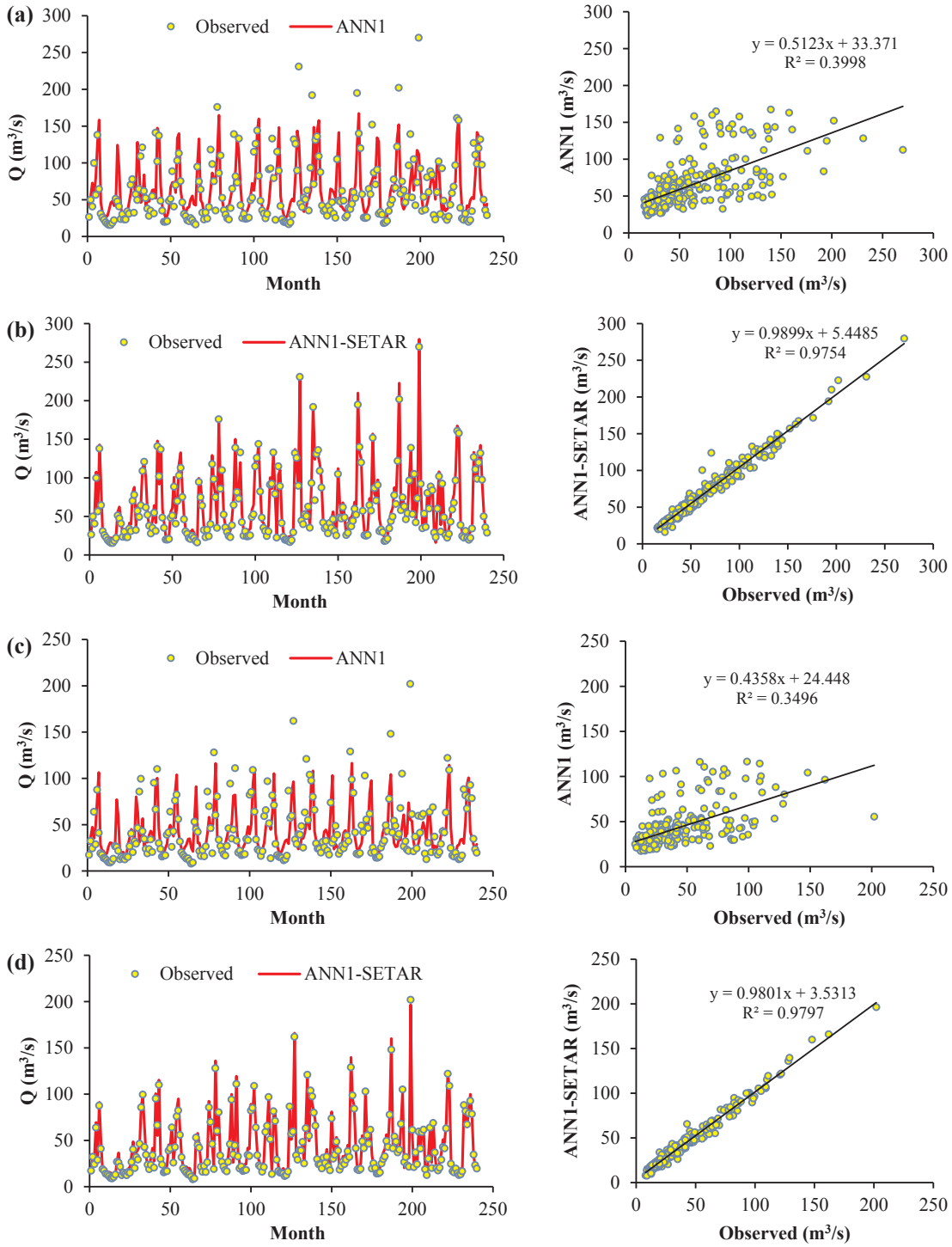

Fig. 7. Comparisons of the observed and predicted monthly river flow data for the superior models of ANN-SETAR and the corresponding ANN models for the test period: (a-b) Brantford, (c-d) Galt.

$$y = f(x) = c_0 + \sum_{i=1}^{M} c_i B_i(x) \tag{4}$$

where y is the dependent variable estimated by the MARS, c_o is a constant, $B_i(x)$ is the ith basis function and c_i is the coefficient of ith basis function where all c_i coefficients are determined by minimizing the sum of square errors.

Fitting the MARS model is executed in two stages consisting of forward and backward stages. In the forward stage, a large number of basis functions with different knots are consecutively added to the model and an over-fitted and complex model is created. In the backward stage, the basis functions which may have less impact on the estimation process are pruned by the MARS. Finally, the optimum MARS model is chosen based on the lowest value of generalized cross validation (GCV) criterion. GCV can be expressed as:

$$GCV(M) = \frac{1}{n} \frac{\sum_{i=1}^{n} [y_i - f(x_i)]^2}{\left(1 - \frac{C(M)}{n}\right)^2} \tag{5}$$

where y_i is the target output, $f(x_i)$ is the estimated output, n is the

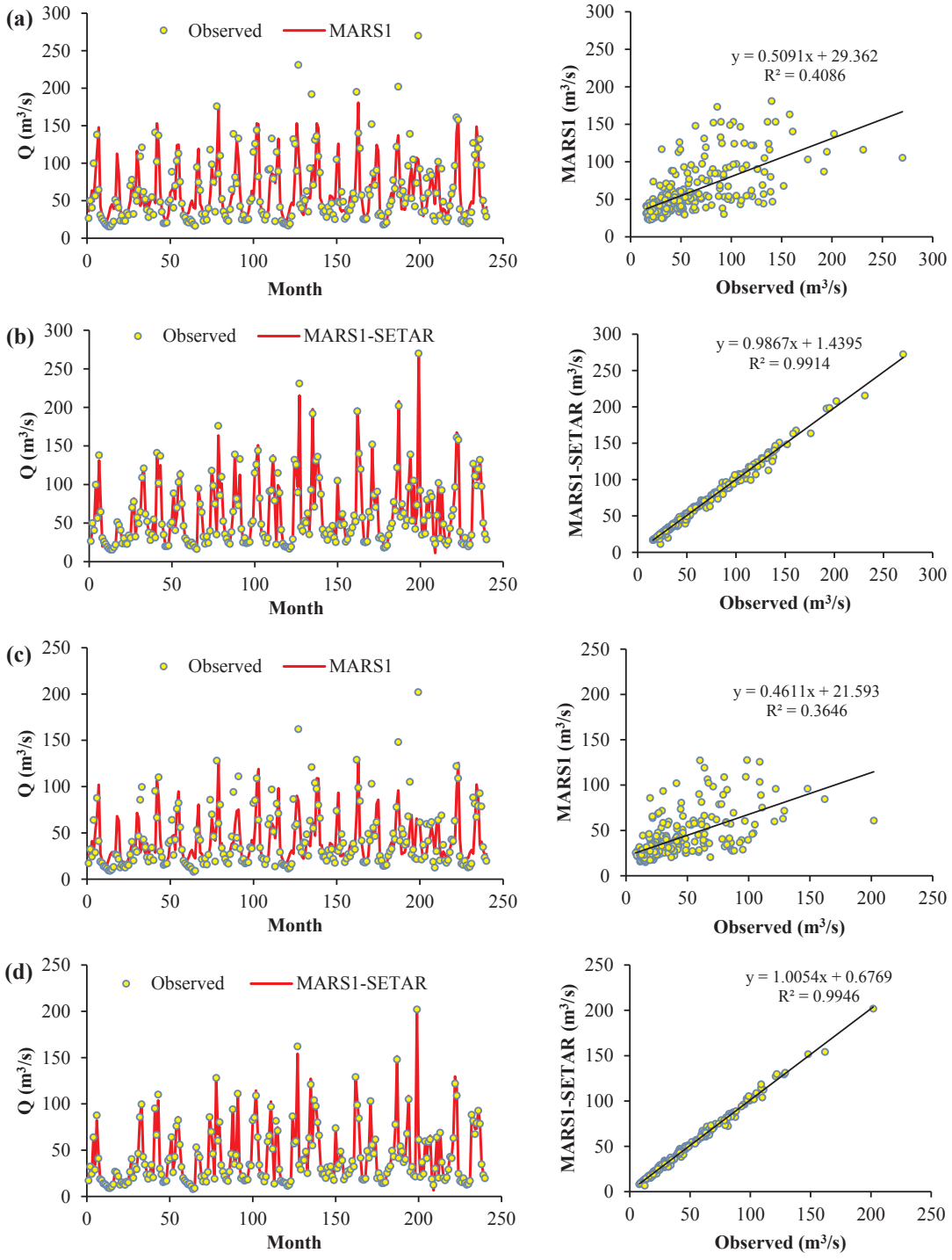

Fig. 8. Comparisons of the observed and predicted monthly river flow data for the superior models of MARS-SETAR and the corresponding MARS models for the test period: (a-b) Brantford, (c-d) Galt.

number of dataset and *C(M)* is a penalty which is defined as:

$$C(M) = (M + 1) + d \times M \quad (6)$$

where M is the number of basis functions and d is a penalty for each basis function involved in the model.

2.4. RF model

The RF as a powerful ensemble-learning algorithm was first introduced by Breiman (2001), which is used for regression analysis, classification, and unsupervised learning purposes (Liaw and Wiener, 2002). The RF algorithm, with the permutation and continuous change of the factors affecting the target variable, leads to the creation of a large number of decision trees, and then all the trees are combined for the prediction. Fig. 5 illustrates a general structure of RF technique. As the number of trees increases, the over-fitting effect that occurs in the decision tree method is eliminated. Thus, at each stage of tree growth, the model is more precise and the error rate decreases. The bagging procedure is applied in the RF to choose the random samples of parameters as the training dataset. Then, for each variable, the function establishes model prediction error if the values of that variable are permuted across the out-of-bag observations (Trigila et al., 2015).

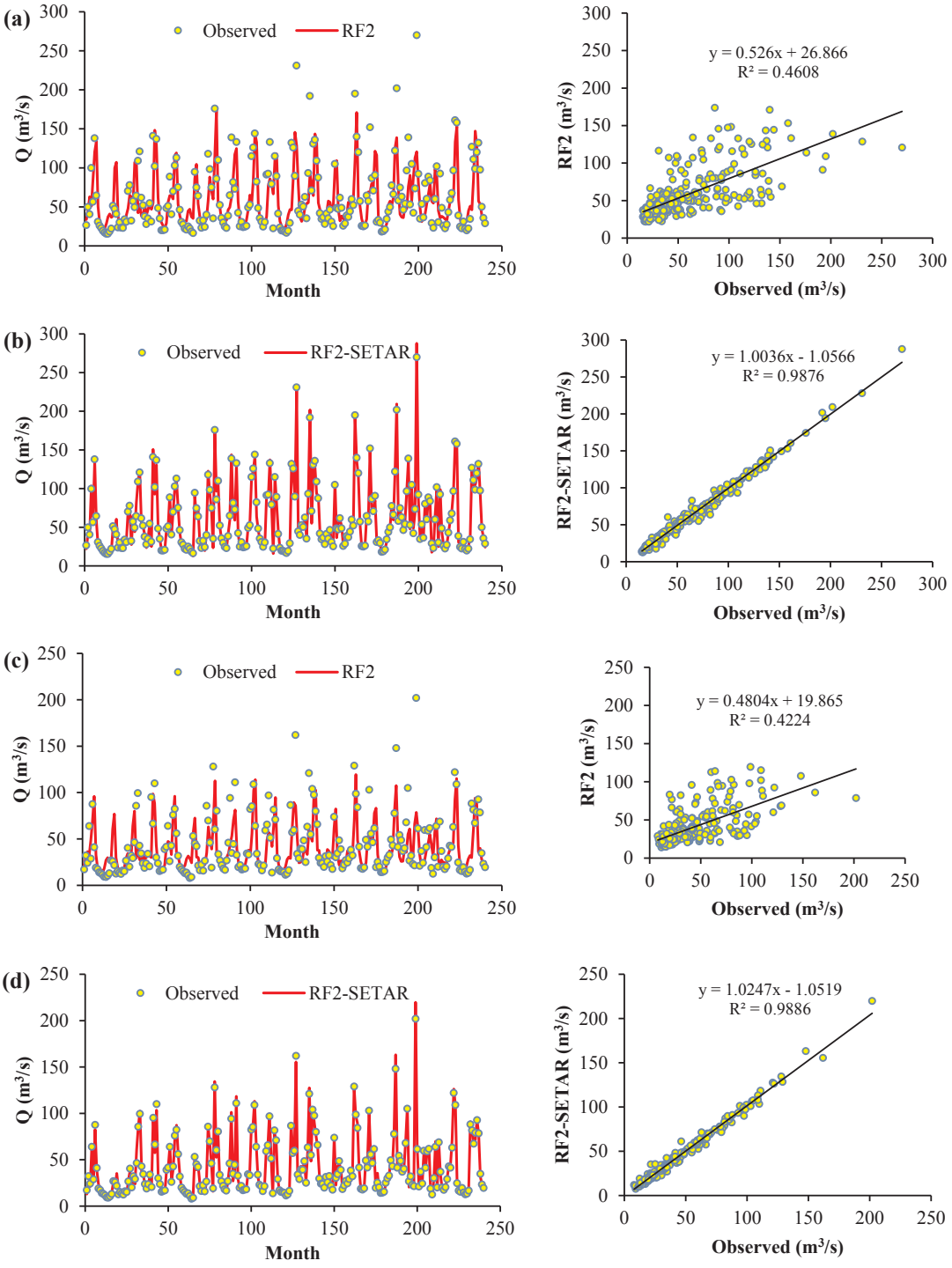

Fig. 9. Comparisons of the observed and predicted monthly river flow data for the superior models of RF-SETAR and the corresponding RF models for the test period: (a-b) Brantford, (c-d) Galt.

Several bootstrap samples of the data are involved in the RF construction. The bootstrap method is a sampling method with permutation. Thus, by repeating the sampling operation, some out-of-bags datasets are created from the training dataset. Out-of-bag predictions are one of the main functions in tuning of the RF for evaluation and generate much faster results in comparison with other methods (Probst et al., 2019).

The number of trees (n_{tree}) is the most important feature of the model that can affect the performance of RF modeling, which is considered as n_{tree} = 500. Furthermore, the number of variables on each node (i.e., m_{try}) is another user-defined parameter of RF implementation. Here, *mtry* = 1 was applied in modeling process. Testing more numbers for trees and variables on each node revealed that n_{tree} = 500 and m_{try} = 1 showed relatively better results.

2.5. SETAR model

One of the non-linear time series model groups is the threshold autoregressive (TAR) models, which are called as a group of non-linear regime-switching approaches. In these types of non-linear time series

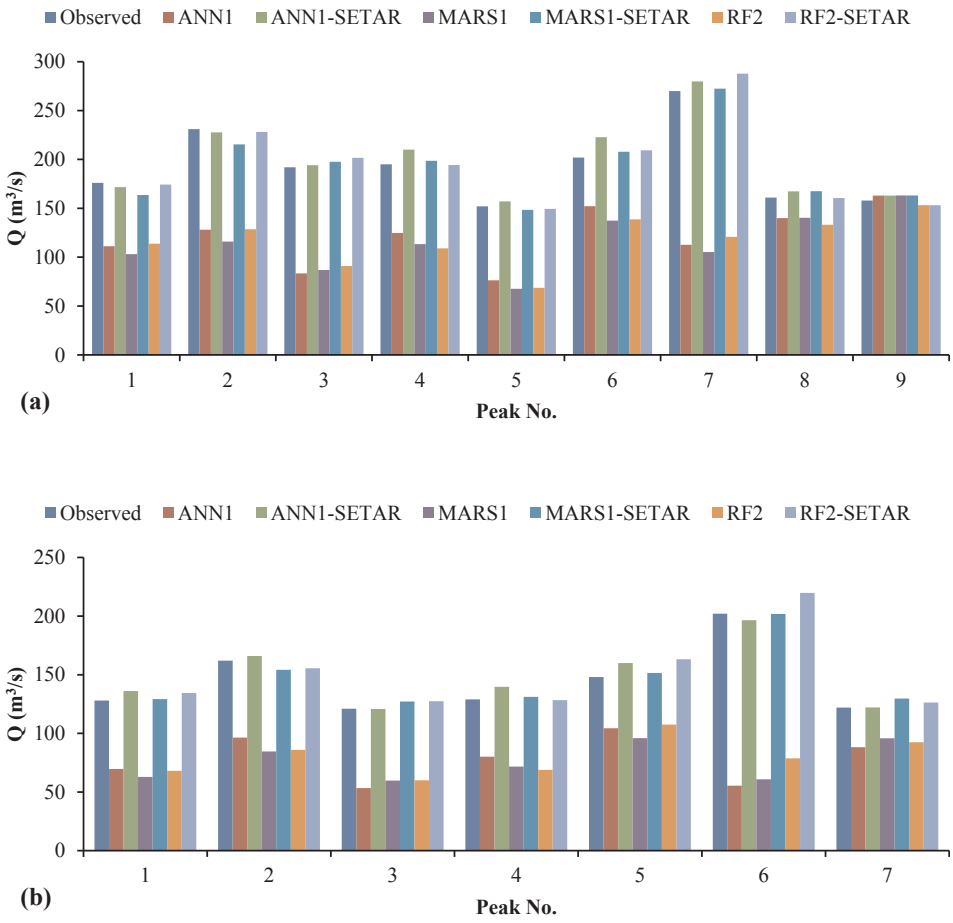

Fig. 10. Comparisons between the observed and predicted peak points of the monthly river flow data for the superior proposed hybrid models and the corresponding stand-alone models during the test period: (a) Brantford, (b) Galt.

models, the time series characteristics consisting of mean, variance, and autocorrelation differ in various regimes (Cryer and Chan, 2008; Tsay, 2010). One of the special cases of the non-linear TAR model is the SETAR model (Tong, 1983) used in the present study. On the basis of TAR-based models structure, a parameter called "threshold" determines the movements of each time series between regimes. The threshold parameter for the SETAR models can be either a given value of the time series used in modeling procedure or a parameter that is determined by an algorithm (Komorník et al., 2006).

If we consider (Y_1, …, Y_n) as the time series dataset for modeling, we can define a two-regime SETAR model, shown as SETAR(p, r) (Cryer and Chan, 2008) as:

$$Y_t = \begin{cases} \varphi_0^{(1)} + \sum_{i=1}^{p} \varphi_i^{(1)} Y_{t-i} + \varepsilon_t^{(1)} & if \;\; Y_{t-d} \le \tau \\ \varphi_0^{(2)} + \sum_{i=1}^{r} \varphi_i^{(2)} Y_{t-i} + \varepsilon_t^{(2)} & if \;\; Y_{t-d} > \tau \end{cases} \quad (7)$$

where n is the length of the time series and φ_i^j ($i \in \{1, 2, ..., p\}$, $i \in \{1, 2, ..., r\}$, $j \in \{1, 2\}$) are the AR models' coefficients. The orders of the lower and upper regimes of the AR models are denoted as p and r respectively, d is as a delay time, τ is the threshold amount (or transition parameter), ε_t is the residual time series at time t, $\varepsilon_t \tilde{N}(0, \sigma^2)$ (Tsay, 2010).

At the first step in modeling procedure of a two-regime SETAR time series model, both the threshold value τ and the lag time parameter d should be determined. The time series dataset, according to the defined limit of each regime ($Y_{t-d} \le \tau$ or not) can be divided into two parts; so that, the data that are smaller or larger than the threshold values are discerned. Finally, for each regime, the same AR model is fitted to each time series dataset detected according to the threshold parameter. By minimizing the Akaike information criterion (AIC) for a fixed τ and d, the orders of the AR model are obtained (Cryer and Chan, 2008) as:

$$\begin{aligned} AIC(p, r, \tau, d) &= -2L(\tau, d) + 2(p + r + 2) \\ L(\tau, d) &= -\tfrac{n-p}{2}\{1 + \log(2\pi)\} - \tfrac{n_1(\tau,d)}{2}\log((\hat{\sigma}_1(\tau, d))^2) \\ &\quad - \tfrac{n_2(\tau,d)}{2}\log((\hat{\sigma}_2(\tau, d))^2) \end{aligned} \quad (8)$$

In this equation, $L(\tau, d)$ is the log-likelihood function that is used to estimate τ and d. The number of observations in each regime are n_1 and n_2 as well as error variances in the lower and upper regimes are $\hat{\sigma}_1$ and $\hat{\sigma}_2$, respectively (Cryer and Chan, 2008).

2.6. GARCH model

The GARCH approach as a non-linear time series model was first suggested by Engle (1982) and then extended by Bollerslev (1986) to model volatility or conditional variance of a univariate time series. In this approach, it is assumed that the obtained residual time series from the model fitted to hydrological time series are dependent upon time. In such conditions, it is expected that variance is not constant over time (conditional time-variant variance); so that, the ARCH efficacy exists in the residuals. In fact, the GARCH approach can describe the trends of conditional variance according to the information of past events. The general structure of a GARCH model can be written as:

$$\sigma_t^2 = Var(\varepsilon_t | \varepsilon_u, u < t) = \omega + \sum_{i=1}^{V} \alpha_i \varepsilon_{t-i}^2 + \sum_{j=1}^{M} \beta_j \sigma_{t-j}^2 \quad (9)$$

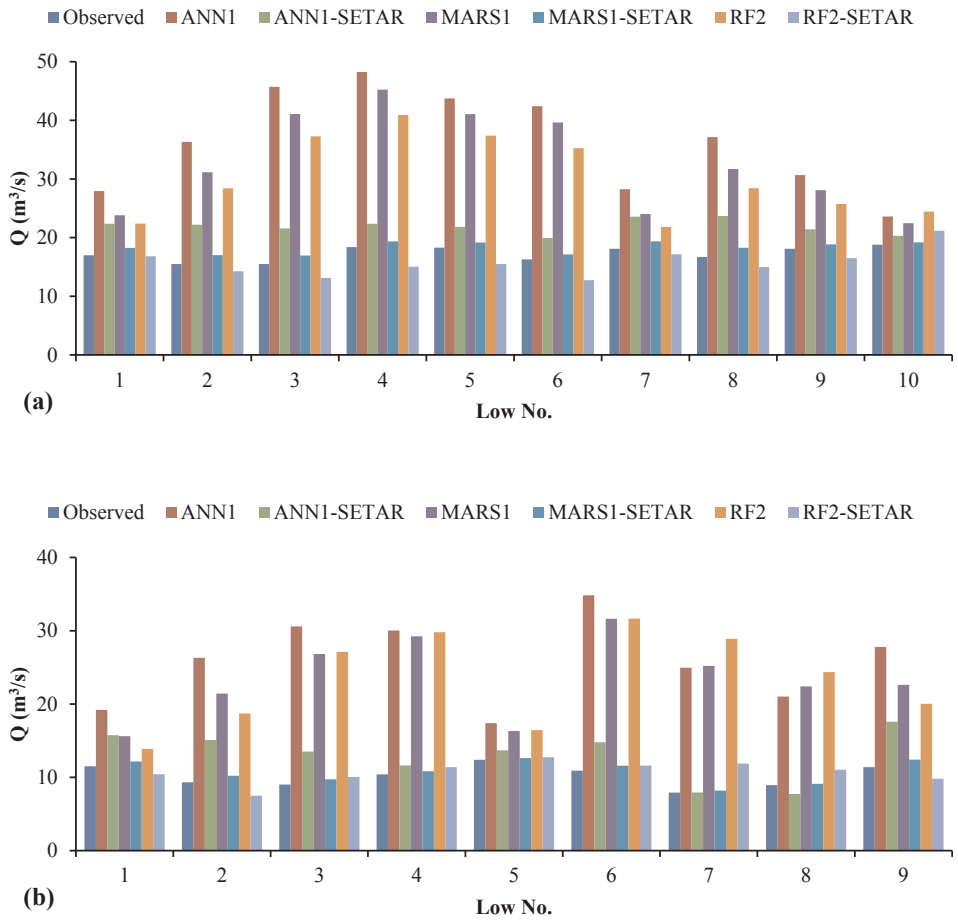

Fig. 11. Comparisons between the observed and predicted low points of the monthly river flow data for the superior proposed hybrid models and the corresponding stand-alone models during the test period: (a) Brantford, (b) Galt.

$$\varepsilon_t = \sigma_t e_t \quad \widetilde{e}_t Normal(0, 1)$$
$$(\varepsilon_t | \psi_{t-1}) Normal(0, \sigma_t^2) \tag{10}$$

where σ_t^2 ($Var(\varepsilon_t|\varepsilon_u, u < t)$) is the conditional heteroscedasticity of the residuals, ω is a constant, α_1, ...,α_V and β_1, ...,β_M are the GARCH model's coefficients as well as the orders of the model's coefficients are V and M. As seen in the GARCH model formula, σ_t^2 value depends on the V past squared residual time series, and the M lagged conditional variance. It should be noted that if $M = 0$, GARCH(V,M) = ARCH(V). The AIC and maximum likelihood estimation (MLE) techniques are used to identify the GARCH model orders and the model's parameters (Cryer and Chan, 2008).

2.7. Coupling the ANN, MARS and RF with SETAR and GARCH models

As mentioned, the main aim of this study is to improve the accuracy of monthly river flow modeling using the ANN, MARS, and RF methods coupled with SETAR and GARCH time series models. Accordingly, the following steps were followed:

1. The deterministic component of the monthly river flow data was predicted using the stand-alone ANN, MARS, and RF models.
2. The optimal SETAR models were fitted to the standardized monthly river flow time series of the two stations to obtain ε_t values.
3. The optimum GARCH model was fitted to the ε_t^2 values obtained from each SETAR model in the previous step.
4. The deterministic component (D_t) of river flow data by the stand-alone ANN, MARS, and RF models was coupled and combined with the stochastic component (S_t) obtained from the SETAR and GARCH models as below:

$$Y_t = D_t + S_t \tag{11}$$

5. The final step was to scale up the obtained Y_t values by de-standardization procedure.

2.8. Evaluation criteria

The performance of stand-alone ANN, MARS, RF, SETAR, GARCH, and hybrid ANN-SETAR, MARS-SETAR, RF-SETAR, ANN-GARCH, MARS-GARCH, and RF-GARCH models was evaluated for predicting the monthly river flow data based on four statistical evaluation indicators. These evaluation criteria include root mean square error (RMSE), mean absolute error (MAE), coefficient of determination (R^2), and Nash-Sutcliffe model efficiency coefficient (E) proposed by Nash and Sutcliffe (1970). These indicators can be defined as:

$$RMSE = \sqrt{\frac{\sum_{i=1}^{N} (Q_{o,i} - Q_{p,i})^2}{N}} \tag{12}$$

$$MAE = \frac{\sum_{i=1}^{N} |Q_{o,i} - Q_{p,i}|}{N} \tag{13}$$

$$R^2 = \left[\frac{\sum_{i=1}^{N} (Q_{o,i} - \bar{Q}_o)\cdot(Q_{p,i} - \bar{Q}_p)}{\sqrt{\sum_{i=1}^{N} (Q_{o,i} - \bar{Q}_o)^2 \cdot \sum_{i=1}^{N} (Q_{p,i} - \bar{Q}_p)^2}} \right]^2 \tag{14}$$

$$E = 1 - \frac{\sum_{i=1}^{N}(Q_{o,i} - Q_{p,i})^2}{\sum_{i=1}^{N}(Q_{o,i} - \bar{Q}_o)^2} \quad (15)$$

where $Q_{o,i}$ and $Q_{p,i}$ are, respectively, the ith observed and predicted monthly river flow, $\bar{Q}_o$ is the mean of observed monthly river flow data, $\bar{Q}_p$ is the mean of predicted monthly river flow data, and N is the number of data in each studied dataset.

3. Results and discussion

3.1. Performance evaluation of the stand-alone and developed hybrid models

The results of fitting the SETAR and GARCH time series models indicated that SETAR(1,1) and GARCH(1,0) are the optimal models fitted to the streamflow datasets of the studied areas. Equations of the optimum SETAR and GARCH models fitted to both of stations are presented in Table 4. Table 5 also illustrates the values of statistical parameters calculated for the optimal SETAR and GARCH time series models for both train and test periods. As seen, the SETAR models developed at Brantford and Galt stations give better accuracies than the GARCH ones. Error indicators of the SETAR models obtained for the test stage are as RMSE = 14.13 m^3/s, MAE = 10.64 m^3/s, R^2 = 0.895, E = 0.894 at Brantford station, and RMSE = 10.25 m^3/s, MAE = 7.59 m^3/s, R^2 = 0.895, E = 0.894 at Galt one.

As previously mentioned in Table 3, one to three months' lagged river flow data in the form of standardized was applied as inputs of the artificial intelligence techniques. These lags were selected based on the auto-correlation functions (ACF) graphs of the standardized data. As clearly seen in Fig. 6, the first three time lags (i.e., Q_{t-1} to Q_{t-3}) demonstrate significant effect on Q_t. The ACF values of other lags are within the confidence intervals. Hence, the first three lags were employed as the inputs in modeling procedure.

As noted, the performance of ANN is affected by the number of neurons in the hidden layer. Various trial and errors for the number of neurons in the hidden layer revealed that their optimal numbers at Brantford station were 2, 2, and 1 for the ANN1, ANN2, and ANN3, respectively. Moreover, the optimal numbers of neurons in the hidden layer at Galt station were 3, 2, and 1, respectively, for the ANN1, ANN2, and ANN3. For example, the structure of ANN2 at Brantford and Galt stations is 2-2-1, which means that the developed ANN respectively contains two, two, and one neurons, in the input, hidden, and output layers (see Fig. 3). Performance evaluation of the stand-alone ANN, MARS, and RF models and their corresponding hybrid models with SETAR and GARCH models are listed in Tables 6 and 7 for both train and test stages at Brantford and Galt stations, respectively. It is obvious from the tables that there are slight differences between the performance of the stand-alone ANN, MARS, and RF models in the scenarios considered for predicting the monthly river flow. However, the MARS and RF models perform slightly better than the ANN at both stations for the scenarios with similar inputs.

In the second part of current research, the results obtained from the stand-alone ANN, MARS, and RF models including the deterministic component of the monthly river flow data were coupled with the outputs of the SETAR and GARCH models. In fact, the SETAR and GARCH models give the stochastic component of the hydrological data such as river flow. Comparing the performance statistics presented in Tables 6 and 7 reveals that the developed hybrid models perform much better than the corresponding stand-alone models. It is clear that the RMSE and MAE statistical evaluation indicators of the stand-alone models are considerably reduced by the proposed hybrid models. Moreover, the values of R^2 and E statistics are significantly improved by the developed hybrid models in comparison with the single models. The performance comparison of hybrid models with each other shows that the ANN-SETAR, MARS-SETAR, and RF-SETAR provide better results than the corresponding ANN-GARCH, MARS-GARCH, and RF-GARCH for river flow modeling. On the other hand, the hybrid RF-SETAR models generally offer the best performance among the developed hybrid models, except for the RF1-SETAR in which the MARS1-SETAR performed the best. The statistical parameters obtained for the best hybrid models during the test period (i.e., MARS1-SETAR) are RMSE = 4.07 m^3/s, MAE = 2.89 m^3/s, R^2 = 0.991 and E = 0.991 at Brantford station as well as RMSE = 2.50 m^3/s, MAE = 1.79 m^3/s, R^2 = 0.995 and E = 0.994 at Galt station.

Performance evaluation of the stand-alone and hybrid models illustrates that the stand-alone SETAR and GARCH have higher accuracies than the stand-alone ANN, MARS and RF. However, the developed hybrid models outperform the stand-alone time series and artificial intelligence models. Figs. 7–9 demonstrate the scatter and time series plots of the observed against predicted river flow data for the superior hybrid and the relevant stand-alone artificial intelligence models. The bolded error values in the Tables 6 and 7 represent the statistics of the best hybrid models at both stations over the test time period. The fitted lines' equations in the scatter plots are in the forms of $y = \alpha_0 x + \alpha_1$ in which y is the predicted river flow, x is the observed river flow, α_0 is the slope and α_1 is the intercept. The intercepts and slopes are closer to 0 and 1, respectively, in the hybrid models than those obtained by the stand-alone models. The lower (close to 0) and higher (close to 1) values for the intercepts and slopes, respectively, can be attributed to the higher values for the R^2 statistic. As clearly seen from the scatter plots, R^2 ranged from 0.9754 in the ANN1-SETAR to 0.9914 in the MARS1-SETAR for Brantford station as well as from 0.9797 in the ANN1-SETAR to 0.9946 in the MARS1-SETAR for Galt station. In addition, the time series plots in Figs. 7–9 reveal that the predicted river flow data are closer to the observed data in the proposed hybrid models compared with the stand-alone ones. Therefore, it can be concluded that the actual fluctuations of river flow time series are well modeled by the hybrid models. Similar results reported by Mehdizadeh et al. (2017, 2018, 2019), Mehdizadeh (2018), Mehdizadeh and Kozekalanai Sales (2018); so that, the hybrid models developed by the combination of artificial intelligence and time series approaches were much more precise in comparison with the single models for modeling the precipitation, reference evapotranspiration, and streamflow processes. In general, a much better performance of the proposed hybrid models can be justified considering the both stochastic and deterministic components of the monthly river flow in the modeling procedure.

It is worthy to mention that over-fitting and curse of dimensionality are crucial problems in artificial intelligence modeling in hydrological science (Safari et al., 2016). To this end, there are number of issues that should be emphasized. Indeed, well-organized models, using large number of data for modelling and existence of stopping criteria (more importantly for ANN) prevent over-fitting (Chang et al., 2010; Srivastava et al., 2014). The over-fitted models perform poorly in the tasting stage, while the developed models in this study provide acceptable results on unseen data set at the testing stage. On the other hand, considering low number of weights with the use of low number of variables in the input of the models decrease the probability of the over-fitting (Bishop, 1995). As it given before, one-three input variables are considered in this study. Moreover, for the case of MARS technique, because of its forward and backward stepwise, unessential variables are removed to prevent over-fitting of the model and increase the model performance (Friedman, 1991, Sharda et al., 2008; Safari, 2019). For the case of RF, over-fitting problem is prevented through its randomness feature (Sadler et al., 2018). ANN model is much less susceptible to the curse of dimensionality (Bishop, 1995). Finally, as developed models are well-organized with large number of data using reliable techniques, it can be said that the developed models in this study were not expected to have such a problem.

3.2. Performance evaluation of the models in predicting extreme values of the monthly river flow data

Having information on the extreme amounts of river flow including peak and low values has a key role in the management of water resources projects and optimal future decisions. Furthermore, the analysis of extreme flows is of particular importance in problems related to water resources management such as dam spillway and sluiceway operations as well as reservoir operation during the drought periods (Sanikhani and Kisi, 2012; Awchi, 2014). Therefore, in this section, the capabilities of the stand-alone and proposed hybrid models were evaluated in predicting peak and low values of river flow data. For this aim, the observed and predicted peak and low values of the monthly river flow data were considered during the test period. It should be noted that the observed river flow values greater than 150 m^3/s and 120 m^3/s were considered as the peaks of the flow data at Brantford and Galt stations, respectively. Moreover, flow rates lower than 19.0 m^3/s and 12.5 m^3/s were chosen as benchmarks at Brantford and Galt stations, respectively, to investigate the performance of stand-alone and hybrid models for estimation of low values of the monthly river flow data.

Comparison of the applied models in predicting peak and low values of the monthly river flow data are made, respectively, in Figs. 10 and 11. As seen in Fig. 10, the single ANN, MARS and RF are not able to predict peak points of the river flow time series at the studied stations. Peak points are under-predicted by the stand-alone models whereas the developed hybrid models can accurately predict peak points of the river flow data. Besides, as obviously seen in Fig. 11, low points of the monthly river flow data are over-predicted by the stand-alone models. Nevertheless, these extreme values can well be modeled in the hybrid models proposed in the present study in comparison with the single ones. As a result, the obtained outcomes confirm that the river flow time series predicted by the developed hybrid models are closely matched to the observed data due to considering the both stochastic and deterministic components.

4. Conclusions

In the present study, an attempt was made to improve the prediction accuracy of monthly river flow at Brantford and Galt stations situated on Grand River, Canada. For this purpose, the various artificial intelligence approaches including ANN, MARS, and RF models were coupled with the SETAR and GARCH time series ones. The acquired results denoted that the hybrid models, namely ANN-SETAR, MARS-SETAR, RF-SETAR, ANN-GARCH, MARS-GARCH, and RF-GARCH outperformed the stand-alone ANN, MARS, RF, SETAR, and GARCH. Nevertheless, the RF-SETAR generally presented the better performance compared with the ANN-SETAR and MARS-SETAR at both stations. The most accurate models among the developed hybrid models of test phase were MARS1-SETAR for both of the considered stations. Error statistics of the RMSE, MAE, R^2, and E obtained for the mentioned model were 4.07 m^3/s, 2.89 m^3/s, 0.991, and 0.991 at Brantford station (Table 6) as well as 2.50 m^3/s, 1.79 m^3/s, 0.995, and 0.994 for Galt station (Table 7). Additionally, the performance of the developed and stand-alone models was investigated for the prediction of extreme values of the monthly river flows. It was concluded that the proposed hybrid models had much better accuracies in predicting the peak and low points of river flows compared with the stand-alone ones. Thus, as a general conclusion, it can be presented that the hybrid models developed in this study can be considered as alternative approaches to the stand-alone artificial intelligence models for precise prediction of the monthly river flow. Additionally, it is suggested that the methodology presented in this study can be used in the future works related to the modeling of other hydrological processes such as rainfall, rainfall-runoff, etc.

Declaration of Competing Interest

The authors declare that there is no conflict of interest.

Acknowledgments

The authors would like to acknowledge Prof. Geoff Syme, Editor-in-Chief, and two anonymous reviewers for their constructive comments that helped us to improve the quality of the paper.

References

Aqil, M., Kita, I., Yano, A., Nishiyama, S., 2007. A comparative study of artificial neural networks and neuro-fuzzy in continuous modeling of the daily and hourly behaviour of runoff. J. Hydrol. 337 (1–2), 22–34.
Awchi, T.A., 2014. River discharges forecasting in Northern Iraq using different ANN techniques. Water Resour. Manage. 28 (3), 801–814.
Babovic, V., 2005. Data mining in hydrology. Hydrol. Proc. An Int. J. 19 (7), 1511–1515.
Bishop, C.M., 1995. Neural Networks for Pattern Recognition. Oxford University Press, U.K.
Bollerslev, T., 1986. Generalized autoregressive conditional heteroskedasticity. J. Econometrics 31 (3), 307–327.
Breiman, L., 2001. Random forests. Mach. Learn. 45, 5–32.
Chang, F.J., Kao, L.S., Kuo, Y.M., Liu, C.W., 2010. Artificial neural networks for estimating regional arsenic concentrations in a blackfoot disease area in Taiwan. J. Hydrol. 388 (1–2), 65–76.
Chau, K.W., Wu, C.L., Li, Y.S., 2005. Comparison of several flood forecasting models in Yangtze River. J. Hydrol. Eng. 10 (6), 485–491.
Cryer, J.D., Chan, K.S., 2008. Time Series Analysis with Applications in R, second ed. Springer, New York.
Di, C., Yang, X., Wang, X., 2014. A four-stage hybrid model for hydrological time series forecasting. PLoS One 8, e104663.
Engle, R.F., 1982. Autoregressive conditional heteroscedasticity with estimates of the variance of United Kingdom inflations. Econometrica 50 (4), 987–1007.
Fathian, F., Fakheri-Fard, A., Ouarda, T.B.M.J., Dinpashoh, Y., Nadoushani, S.S.M., 2019. Multiple streamflow time series modeling using VAR–MGARCH approach. Stoch. Environ. Res. Risk Assess. 33 (2), 407–425.
Friedman, J.H., 1991. Multivariate adaptive regression splines. Ann. Stat. 19, 1–67.
Gershenfeld, N.A., Weigend, A.S., 1994. Time series prediction: forecasting the future and understanding the past. In: Weigend, A.S., Gershenfeld, N.A. (Eds.), The Future of Time Series. Addison-Wesley, Reading, MA, pp. 161–163 1-70, Int. J. Forecas.10 (1).
Ghorbani, M.A., Ahmad Zadeh, H., Isazadeh, M., Terzi, O., 2016a. A comparative study of artificial neural network (MLP, RBF) and support vector machine models for river flow prediction. Environ. Earth Sci. https://doi.org/10.1007/s12665-015-5096-x.
Ghorbani, M.A., Khatibi, R., Goel, A., FazeliFard, M.H., Azani, A., 2016b. Modeling river discharge time series using support vector machine and artificial neural networks. Environ. Earth Sci. https://doi.org/10.1007/s12665-016-5435-6.
He, Z., Wen, X., Liu, H., Du, J., 2014. A comparative study of artificial neural network, adaptive neuro fuzzy inference system and support vector machine for forecasting river flow in the semiarid mountain region. J. Hydrol. 509, 379–386.
Kalteh, A.M., 2013. Monthly river flow forecasting using artificial neural network and support vector regression models coupled with wavelet transform. Comput. Geosci. 54, 1–8.
Kisi, O., Cimen, M., 2011. A wavelet-support vector machine conjunction model for monthly streamflow forecasting. J. Hydrol. 399 (1–2), 132–140.
Komorník, J., Komorníková, M., Mesiar, R., Szökeová, D., Szolgay, J., 2006. Comparison of forecasting performance of nonlinear models of hydrological time series. Phys. Chem. Earth A/B/C 31 (18), 1127–1145.
Liaw, A., Wiener, M., 2002. Classification and regression by random forest. R News 2 (3), 18–22.
Mehdizadeh, S., Behmanesh, J., Khalili, K., 2017. A comparison of monthly precipitation point estimates using integration of soft computing methods and GARCH time series model. J. Hydrol. 554, 721–742.
Mehdizadeh, S., 2018. Estimation of daily reference evapotranspiration (ET_o) using artificial intelligence methods: offering a new approach for lagged ET_o data-based modeling. J. Hydrol. 559, 794–812.
Mehdizadeh, S., Kozekalani Sales, A., 2018. A comparative study of autoregressive, autoregressive moving average, gene expression programming and Bayesian networks for estimating monthly streamflow. Water Resour. Manage. 32 (9), 3001–3022.
Mehdizadeh, S., Behmanesh, J., Khalili, K., 2018. New approaches for estimation of monthly rainfall based on GEP-ARCH and ANN-ARCH hybrid models. Water Resour. Manage. 32 (2), 527–545.
Mehdizadeh, S., Fathian, F., Adamowski, J.F., 2019. Novel hybrid artificial intelligence-time series models for monthly streamflow modeling. Appl. Soft Comput. https://doi.org/10.1016/j.asoc.2019.03.046.
Modarres, R., Ouarda, T.B.M.J., 2013. Modeling rainfall–runoff relationship using multivariate GARCH model. J. Hydrol. 499, 1–18.
Moeeni, H., Bonakdari, H., Ebtehaj, I., 2017. Integrated SARIMA with neuro-fuzzy systems and neural networks for monthly inflow prediction. Water Resour. Manage. 31 (7), 2141–2156.
Nash, J.E., Sutcliffe, J.V., 1970. River flow forecasting through conceptual models part I—A discussion of principles. J. Hydrol. 10 (3), 282–290.

Nayak, P.C., Sudheer, K.P., Rangan, D.M., Ramasastri, K.S., 2005. Short-term flood forecasting with a neurofuzzy model. Water Resour. Res. 41 (4), 2517–2530.
Peueot, C., Cappelaere, B., Vieux, B.E., Seguis, L., Maia, A., 2003. Hydrologic process simulation of a semiarid, endorheic catchment in Sahelian West Niger. 1. Model-aided data analysis and screening. J. Hydrol. 279, 224–243.
Probst, P., Wright, M.N., Boulesteix, A.L., 2019. Hyperparameters and tuning strategies for random forest. Wiley Interdiscip. Rev. Data Min. Knowledge Discov. 9 (3), e1301.
Ravansalar, M., Rajaee, T., Kisi, O., 2017. Wavelet-linear genetic programming: a new approach for modeling monthly streamflow. J. Hydrol. 549, 461–475.
Sadler, J.M., Goodall, J.L., Morsy, M.M., Spencer, K., 2018. Modeling urban coastal flood severity from crowd-sourced flood reports using poisson regression and random forest. J. Hydrol. 559, 43–55.
Safari, M.J.S., Aksoy, H., Mohammadi, M., 2016. Artificial neural network and regression models for flow velocity at sediment incipient deposition. J. Hydrol. 541, 1420–1429.
Safari, M.J.S., 2019. Decision tree (DT), generalized regression neural network (GR) and multivariate adaptive regression splines (MARS) models for sediment transport in sewer pipes. Water Sci. Technol. 79 (6), 1113–1122.
Samsudin, R., Saad, P., Shabri, A., 2011. River flow time series using least squares support vector machines. Hydrol. Earth Syst. Sci. 15, 1835–1852.
Sanikhani, H., Kisi, O., 2012. River flow estimation and forecasting by using two different adaptive neuro-fuzzy approaches. Water Resour. Manage. 26 (6), 1715–1729.
Sharda, V.N., Prasher, S.O., Patel, R.M., Ojasvi, P.R., Prakash, C., 2008. Performance of Multivariate Adaptive Regression Splines (MARS) in predicting runoff in mid-Himalayan micro-watersheds with limited data. Hydrol. Sci. J. 53 (6), 1165–1175.
Srivastava, N., Hinton, G., Krizhevsky, A., Sutskever, I., Salakhutdinov, R., 2014. Dropout: a simple way to prevent neural networks from overfitting. The J. Mach. Learn. Res. 15 (1), 1929–1958.
Terzi, O., Ergin, G., 2014. Forecasting of monthly river flow with autoregressive modeling and data-driven techniques. Neural Comput. Appl. 25 (1), 179–188.
Tong, H., 1983. Threshold Models in Non-linear Time Series Analysis. Springer, New York.
Trigila, A., Iadanza, C., Esposito, C., Scarascia-Mugnozza, G., 2015. Comparison of logistic regression and random forests techniques for shallow landslide susceptibility assessment in Giampilieri (NE Sicily, Italy). Geomorphology 249, 119–136.
Tsay, R.S., 2010. Analysis of Financial Time Series, 3rd ed. John Wiley & Sons Inc, Hoboken, NJ.
Wu, C.L., Chau, K.W., Li, Y.S., 2009. Predicting monthly streamflow using data-driven models coupled with data-preprocessing techniques. Water Resour. Res. 45 (8), W08432.
Yaseen, Z.M., Jaafar, O., Deo, R.C., Kisi, O., Adamowski, J., Quilty, J., El-Shafie, A., 2016a. Boost stream-flow forecasting model with extreme learning machine data-driven: a case study in a semi-arid region in Iraq. J. Hydrol. 542, 603–614.
Yaseen, Z.M., El-Shafie, A., Afan, H.A., Hameed, M., Mohtar, W.H.M.W., Hussain, A., 2016b. RBFNN versus FFNN for daily river flow forecasting at Johor River, Malaysia. Neural Comput. Appl. 27 (6), 1533–1542.
Yu, X., Liong, S.Y., Babovic, V., 2004. EC-SVM approach for real-time hydrologic forecasting. J. Hydroinform. 6 (3), 209–223.
Zhang, H., Singh, V.P., Wang, B., Yu, Y., 2016. CEREF: a hybrid data-driven model for forecasting annual streamflow from a socio-hydrological system. J. Hydrol. 540, 246–256.